

Merits concerning energy-consumption and trajectory-tracking accuracy derived from elbow-bracing robot

Xiang LI*, Keli SHEN* and Mamoru MINAMI*

* Graduate School of Nature Science and Technology, Okayama University
3-1-1 Tsushima-naka, Kita-ku, Okayama-shi, Okayama-ken, 700-8530, Japan
E-mail: pzkm87r2@s.okayama-u.ac.jp

Received: 13 April 2017; Revised: 15 July 2017; Accepted: 10 October 2017

Abstract

Considering that humans perform handwriting task with reduced powers by contacting elbow or wrist on a table, it is reasonable to deem that manipulators can save energy and simultaneously accomplish writing tasks precisely like humans by bracing intermediate links such as elbow or wrist. First this paper discusses equation of motion of robot under bracing constraint condition, based on the robot's dynamics with constraint condition including motor dynamics. Then a control method to utilize the constraint dynamics is proposed to control simultaneously bracing force and hand's trajectory in work space. Even though the model used for the simulation analyses is simple four-links manipulator, the simple structure can help understand even more clearly the effects got by bracing part of the manipulator. This paper demonstrates the merits of the strategy to utilize bracing by comparing the contacting motions with non-contacting motions, including ; (1) the energy consumption can be reduced; (2) the hand trajectory tracking becomes accurate; (3) there is an optimum contacting point that minimize the energy consumption on condition that trajectory-tracking task be given to the hand.

Keywords : Bracing manipulator, Energy-consumption, Constraint motion, Trajectory-tracking accuracy, Numerical simulation

1. Introduction

Kinematical considerations on control methods for redundant manipulators have been researched widely and the effectiveness was explained by Chirikjian and Burdick scrupulously in (Chirikjian and Burdick, 1994) Hyper-redundant manipulators can variedly change the configuration through the use of redundancy, where "change the configuration" means that the shape of manipulator is changed while the hand pose (position and orientation) is controlled to desired one. On the other hand the weight of manipulators with high redundancy increases as the number of links increases, which causes the lifting capacity of the hand be lessened.

In many researches, methods of using redundancy for obstacle avoidance (Glass, et al, 1995), (Seraji and Bon, 1999) and optimization of configuration (Hirose and Chu, 1999) were discussed, and have been used practically in factories. But hyper-redundant manipulators deem that they do not reach practical level at present stage since the lifting capacity of hand is decreased meaninglessly as the redundancy degree increases, and what to be the worst in this case is that the increase of robot's whole weight is inevitable. This leads the conclusion that the hyper-redundant manipulator is not realistic for industrial use. The research direction of this paper has been set for solving the problem about the redundant manipulators above mentioned.

Humans can write characters on a paper at will with less power by bracing and restricting the wrist, as shown in Fig.1. Redundant manipulators seem to have possibilities to operate accurately with less energy by bracing elbow on environments like humans' writing behaviours, and this bracing strategy may overcome the hindrances of hyper-redundant manipulators being too heavy to spare the hand payload for desired tasks.



Fig. 1 Human's writing motion utilizing bracing wrist

Roy and Whitcomb (2002) categorized motions and control methods of constrained robot as (a) model based control (Siciliano and Villani, 1996), (Villani, de Wit and Brogliato, 1999) that assumes undeformable robots and deformable environments, and (b) methods based on position/velocity control (Schutter and Brussel, 1988) that assumes undeformable robots and also deformable environments. Park and Khatib (2005), (2007) proposed kinematics model of plural contacts to control constraint motion in category (b). Finally, there is classification of (c) control method (Yoshikawa, 1987) that assumes undeformable robots and undeformable environments. Yamane and Nakamura proposed walking of humanoid robot (Yamane and Nakamura, 2001) and a concept of dynamics filter (Yamane and Nakamura, 2001) in this category. Effectiveness and accuracy of hyper-redundant manipulators subject to constraint on environments in category (c) have been discussed, West and Asada (1985) proposed common contact mode of kinematics for designing position/force simultaneous controller of manipulator in constraint motion.

In this paper, the control method in (c) of undeformable robots and undeformable environments is discussed. Under the conditions, algebraic equation can be derived from constraint condition and equation of motion as Eq.(1).

$$\mathbf{A}\mathbf{f}_n = \mathbf{a} - \mathbf{B}\boldsymbol{\tau} \quad (1)$$

\mathbf{f}_n is a vector of constraint force, \mathbf{a} , \mathbf{A} and \mathbf{B} are vector and matrices that will be defined in the next chapter, $\boldsymbol{\tau}$ is a vector of input torques. Eq.(1) shows that an algebraic relation between input torques and constraint force reins the motion when robot's hand is subject to constraint. The above equation has been derived by Hemami and Wyman (1979) in dynamical modeling of biped walking when lifting leg contacting with floor, and applied by Peng and Adachi (1991) for force/position control by robots at the beginning. Peng considered that $\boldsymbol{\tau}$ is input and \mathbf{f}_n is output, and Eq.(1) was used as force sensor to detect \mathbf{f}_n .

Despite the nature that the robot motions under a condition of (c) — undeformable robot and undeformable environment — be subject to the algebraic equation that is Eq.(1), researches on robot force control in category (c) seems to be not based on the Eq.(1) except Peng as far as we know. What we want to emphasize is that the transfer from $\boldsymbol{\tau}$ to \mathbf{f}_n is instant as shown in Eq.(1), unlike the dynamical relations of position and velocity, since it is algebraic relation.

In this paper, Eq.(1) is used for calculating input torque $\boldsymbol{\tau}$ to accomplish desired constraint force \mathbf{f}_{nd} contrary to Peng's idea. Considering the hand writing motion, it is clear that too much pushing the wrist to table bears fatigue and meaningless, and also too less supporting the wrist makes us tired too. This suggests a hypothesis that appropriate supporting force exists, and also effective bracing position may exist.

In the past of our researches, the control of constraint motion has been applied to robots. Minami proposed force control strategy in (Minami, et al., 1997), which was developed into real grinding experiment and extended into shape-grinding (Minami and Xu, 2008), (Minami, et al., 2014) — grinding a target object into desired shape with force-sensorless feed-forward control based on Eq.(1). The bracing control also was used to a mobile robot with redundant manipulator mounted on a mobile robot (Washino, et al., 2012) and Kondo (2013) proposed a strategy to save energy of the redundant manipulator.

In this paper, the effectiveness of bracing is discussed intensively from some new view points unlike previous researches (Kondo, et al., 2013), including the effectiveness of hand trajectory tracking precision in comparison between elbow bracing condition and no-bracing condition, and dependence of the initial states on the tracking errors.

The purpose of this research is to analyze effectiveness of constraint motion on the view points of trajectory tracking performances of the hand and energy consumption efficiency. The optimization of bracing position based on minimization criterion of energy consumption has been discussed through analyzing relations between bracing position, hand trajectory and hand's payload.

2. Modeling of Constraint Manipulator

2.1. Constraint Motion with Bracing Elbow

In this section, a dynamical model of an elbow-bracing robot that contacts multiple points with environments is discussed. Considering conditions that intermediate links of an n -link manipulator are being subject to multiple constraints at p points, the constraint is expressed as,

$$\begin{aligned} \mathbf{C}(\mathbf{q}) &= [C_1(\mathbf{r}_1(\mathbf{q})), C_2(\mathbf{r}_2(\mathbf{q})), \dots, C_p(\mathbf{r}_p(\mathbf{q}))]^T \\ &= \mathbf{0}. \end{aligned} \quad (2)$$

Here, $\mathbf{q} \in \mathbf{R}^n$ is joint angle vector with n joints, $\mathbf{r}_i \in \mathbf{R}^m (m < n, i = 2, \dots, n-2)$ is i -th link position. The relations between \mathbf{r}_i and \mathbf{q} and between $\dot{\mathbf{r}}_i$ and $\dot{\mathbf{q}}$ are expressed as,

$$\mathbf{r}_i = \mathbf{r}_i(\mathbf{q}), \quad (3)$$

$$\dot{\mathbf{r}}_i = \mathbf{J}_i(\mathbf{q})\dot{\mathbf{q}}, \quad \mathbf{J}_i(\mathbf{q}) = [\tilde{\mathbf{J}}_i(\mathbf{q}), \mathbf{0}]. \quad (4)$$

In Eq.(4), \mathbf{J}_i is $m \times n$ Jacobian matrix, $\tilde{\mathbf{J}}_i$ consists of $m \times i$ matrix and zero submatrix $\mathbf{0}$ with $m \times (n-i)$.

Assuming that a plural intermediate links are contacting with environment whose constraint condition is $C_i(\mathbf{r}_i) = 0$, the $n \times 1$ column vectors that represent influence to joint space of constraint forces and friction forces concerning C_i are

$$\left(\frac{\partial C_i}{\partial \mathbf{q}^T} \right)^T / \left\| \frac{\partial C_i}{\partial \mathbf{r}^T} \right\| = \mathbf{j}_{ci}^T, \quad (5)$$

$$\left(\frac{\partial \mathbf{r}_i}{\partial \mathbf{q}^T} \right)^T \frac{\dot{\mathbf{r}}_i}{\|\dot{\mathbf{r}}_i\|} = \mathbf{j}_{ii}^T. \quad (6)$$

$\mathbf{J}_c^T, \mathbf{J}_i^T, \mathbf{f}_n$ and \mathbf{f}_i are defined as

$$\mathbf{J}_c^T = [\mathbf{j}_{c1}^T, \mathbf{j}_{c2}^T, \dots, \mathbf{j}_{cp}^T], \quad (7)$$

$$\mathbf{J}_i^T = [\mathbf{j}_{i1}^T, \mathbf{j}_{i2}^T, \dots, \mathbf{j}_{ip}^T], \quad (8)$$

$$\mathbf{f}_n = [f_{n1}, f_{n2}, \dots, f_{np}]^T, \quad (9)$$

$$\mathbf{f}_i = [f_{i1}, f_{i2}, \dots, f_{ip}]^T. \quad (10)$$

$\mathbf{J}_c^T, \mathbf{J}_i^T$ are $n \times p$ matrices, and the normal force \mathbf{f}_n , frictional force \mathbf{f}_i are $p \times 1$ vectors. Using above definitions, equation of motion of the manipulator subject to constraints at p points is expressed as

$$\begin{aligned} \mathbf{M}(\mathbf{q})\ddot{\mathbf{q}} + \mathbf{h}(\mathbf{q}, \dot{\mathbf{q}}) + \mathbf{g}(\mathbf{q}) + \mathbf{D}\dot{\mathbf{q}} \\ = \boldsymbol{\tau} + \sum_{i=1}^p (\mathbf{j}_{ci}^T f_{ni}) - \sum_{i=1}^p (\mathbf{j}_{ii}^T f_{ii}) \\ = \boldsymbol{\tau} + \mathbf{J}_c^T \mathbf{f}_n - \mathbf{J}_i^T \mathbf{f}_i. \end{aligned} \quad (11)$$

Here, \mathbf{M} is inertia matrix, \mathbf{h} is centrifugal force and Coriolis force, \mathbf{g} is gravity and \mathbf{D} means viscous friction.

Differentiating Eq.(2) with respect to time t twice, constraint condition of $\ddot{\mathbf{q}}$ is set up like

$$\dot{\mathbf{q}}^T \left[\frac{\partial}{\partial \mathbf{q}} \left(\frac{\partial \mathbf{C}}{\partial \mathbf{q}^T} \right) \right] \dot{\mathbf{q}} + \left(\frac{\partial \mathbf{C}}{\partial \mathbf{q}^T} \right) \ddot{\mathbf{q}} = \mathbf{0}. \quad (12)$$

The solutions of Eq.(11), $\dot{\mathbf{q}}$ and \mathbf{q} , must satisfy Eq.(2) disregarding time t , meaning that the manipulator be always subject to constraints. Given that the $\ddot{\mathbf{q}}$ satisfying Eq.(12) and the $\ddot{\mathbf{q}}$ in Eq.(11) are identical to each other, the solution $\mathbf{q}(t)$ in Eq.(11) satisfies Eq.(2) regardless of time.

Here, the relation between constraint force \mathbf{f}_n and friction force \mathbf{f}_i is related by the following equation with sliding friction coefficients K_i .

$$\mathbf{f}_i = \mathbf{K} \mathbf{f}_n, \quad \mathbf{K} = \text{diag}[K_1, K_2, \dots, K_p] \quad (13)$$

$$0 < K_i < 1, (i = 1, 2, \dots, p)$$

Therefore, Eq.(11) translates into the following equation.

$$\mathbf{M}(\mathbf{q})\ddot{\mathbf{q}} + \mathbf{h}(\mathbf{q}, \dot{\mathbf{q}}) + \mathbf{g}(\mathbf{q}) + \mathbf{D}\dot{\mathbf{q}} = \boldsymbol{\tau} + (\mathbf{J}_c^T - \mathbf{J}_i^T \mathbf{K}) \mathbf{f}_n \quad (14)$$

2.2. Derivation of Reaction Force with Elbow-Bracing

The derivation of Eq.(1) is discussed here. First, eliminating $\ddot{\mathbf{q}}$ by using Eqs.(11) and (12), and defining $(\partial\mathbf{C}/\partial\mathbf{q}^T)\mathbf{M}^{-1}(\partial\mathbf{C}/\partial\mathbf{q}^T)^T$ as \mathbf{M}_c , the following equation is derived.

$$\begin{aligned} \mathbf{M}_c\mathbf{P}\mathbf{f}_n &= \left(\frac{\partial\mathbf{C}}{\partial\mathbf{q}^T}\right)\mathbf{M}^{-1}(\mathbf{J}_t^T\mathbf{K}\mathbf{f}_n + \mathbf{D}\dot{\mathbf{q}} + \mathbf{h} + \mathbf{g} - \boldsymbol{\tau}) \\ &\quad - \dot{\mathbf{q}}^T \left[\frac{\partial}{\partial\mathbf{q}} \left(\frac{\partial\mathbf{C}}{\partial\mathbf{q}^T} \right) \right] \dot{\mathbf{q}} \end{aligned} \quad (15)$$

Where $\mathbf{P} = \text{diag}[1/\|\partial\mathbf{C}_1/\partial\mathbf{r}^T\|, \dots, 1/\|\partial\mathbf{C}_p/\partial\mathbf{r}^T\|]$. Moreover, by using following definitions,

$$\mathbf{B} = \left(\frac{\partial\mathbf{C}}{\partial\mathbf{q}^T}\right)\mathbf{M}^{-1}, \quad (16)$$

$$\mathbf{a} = \mathbf{B}\{\mathbf{D}\dot{\mathbf{q}} + \mathbf{h} + \mathbf{g}\} - \dot{\mathbf{q}}^T \left[\frac{\partial}{\partial\mathbf{q}} \left(\frac{\partial\mathbf{C}}{\partial\mathbf{q}^T} \right) \right] \dot{\mathbf{q}}, \quad (17)$$

Eq.(15) can be translated into,

$$\mathbf{M}_c\mathbf{P}\mathbf{f}_n = \mathbf{B}\mathbf{J}_t^T\mathbf{K}\mathbf{f}_n - \mathbf{B}\boldsymbol{\tau} + \mathbf{a}. \quad (18)$$

By defining the following matrix \mathbf{A} ,

$$\mathbf{A} = \mathbf{M}_c\mathbf{P} - \mathbf{B}\mathbf{J}_t^T\mathbf{K}. \quad (19)$$

and by inputting Eq.(19) to Eq.(18), Eq.(1) has been derived. The relation between constraint force \mathbf{f}_n and input torque $\boldsymbol{\tau}$ is expressed as algebraic equation. Because \mathbf{f}_n is p dimension vector and $\boldsymbol{\tau}$ is n dimension vector, $\boldsymbol{\tau}$ that achieves \mathbf{f}_n has constraint redundancy. How to use this constraint redundancy will be discussed in the following section 3.

2.3. Equation of Motion of Robot with Motor

Currents of motors are expressed as a vector \mathbf{i} . By putting a dynamics of motor into Eq.(14), the following equation is gotten,

$$\begin{aligned} &(\mathbf{M}(\mathbf{q}) + \mathbf{J}_m)\ddot{\mathbf{q}} + \mathbf{h}(\mathbf{q}, \dot{\mathbf{q}}) + \mathbf{g}(\mathbf{q}) + (\mathbf{D} + \mathbf{D}_m)\dot{\mathbf{q}} \\ &= \mathbf{K}_m\mathbf{i} + (\mathbf{J}_c^T - \mathbf{J}_t^T\mathbf{K})\mathbf{f}_n. \end{aligned} \quad (20)$$

Here, \mathbf{J}_m is a diagonal matrix of inertia moment of motors' rotors, \mathbf{D}_m is a coefficient matrix of viscosity resistance, \mathbf{K}_m is a torque constant matrix of motors.

The relation between applied voltage and current of motor is expressed as

$$\mathbf{L}\frac{d\mathbf{i}}{dt} = \mathbf{v} - \mathbf{R}\mathbf{i} - \mathbf{K}_m\dot{\mathbf{q}}. \quad (21)$$

Eq.(21) is combined with Eqs.(12), (20), where \mathbf{L} is inductance matrix, \mathbf{R} is resistance matrix of motor, and \mathbf{v} is applied voltage to motors. So, equation of motion including the dynamics of motor of n links manipulator that is subject to constraints at p points are expressed as

$$\begin{aligned} &\begin{bmatrix} \mathbf{M} + \mathbf{J}_m & -(\mathbf{J}_c^T - \mathbf{J}_t^T\mathbf{K}) & \mathbf{0} \\ \frac{\partial\mathbf{C}}{\partial\mathbf{q}^T} & \mathbf{0} & \mathbf{0} \\ \mathbf{0} & \mathbf{0} & \mathbf{L} \end{bmatrix} \begin{bmatrix} \ddot{\mathbf{q}} \\ \mathbf{f}_n \\ d\mathbf{i}/dt \end{bmatrix} \\ &= \begin{bmatrix} \mathbf{K}_m\mathbf{i} - \mathbf{h} - \mathbf{g} - (\mathbf{D} + \mathbf{D}_m)\dot{\mathbf{q}} \\ -\dot{\mathbf{q}}^T \left[\frac{\partial}{\partial\mathbf{q}} \left(\frac{\partial\mathbf{C}}{\partial\mathbf{q}^T} \right) \right] \dot{\mathbf{q}} \\ \mathbf{v} - \mathbf{R}\mathbf{i} - \mathbf{K}_m\dot{\mathbf{q}} \end{bmatrix}. \end{aligned} \quad (22)$$

3. Position/Force Control to Use Constraint Redundancy

Hereafter the robot used in this paper is assumed to be a 4-link manipulator that moves in sagittal plane with the second link being braced against floor. When the torque $\boldsymbol{\tau} = [\tau_1, \tau_2, \tau_3, \tau_4]^T$ can be input to joints, the solution $\boldsymbol{\tau}$ of Eq.(1) that achieves desired constraint force f_{n2d} is expressed as

$$\boldsymbol{\tau} = \mathbf{B}^+(\mathbf{a} - \mathbf{A}f_{n2d}) + (\mathbf{I} - \mathbf{B}^+\mathbf{B})\boldsymbol{p}. \quad (23)$$

The $\mathbf{B}^+(4 \times 1)$ is pseudo inverse matrix whose rank be 1, then $\text{rank}(\mathbf{I} - \mathbf{B}^+\mathbf{B})$ is equal to 3. Because $\mathbf{I} - \mathbf{B}^+\mathbf{B}$ is non-dimensional matrix, \boldsymbol{p} has dimensions of torque. Considering \boldsymbol{p} to be new input, \boldsymbol{p} can be used to track target trajectory of hand \mathbf{r}_d and control bracing position through null-space $\mathbf{I} - \mathbf{B}^+\mathbf{B}$ of \mathbf{B} . By the nature of pseudo inverse matrix, adding any value to \boldsymbol{p} has no influences on achieving desired constraint force of 2nd link, f_{n2d} . So, the task of tracking trajectory and the task of controlling f_{n2} as reaction force can be achieved in decoupled manner.

Here, a method to determine \boldsymbol{p} is discussed. In the simulation to utilize four-link manipulator with 2nd link bracing in this report, one degree of freedom is used for force control of elbow, then other one degree can be used for contacting position control of elbow and two remaining degrees can be used for two-dimensional position control of hand.

$$\begin{aligned} \boldsymbol{p} = & \tilde{\mathbf{J}}_{2y}^T [K_{p2y}(y_{d2} - y_2) + K_{d2y}(\dot{y}_{d2} - \dot{y}_2)] \\ & + \mathbf{J}_4^T [\mathbf{K}_{p4}(\mathbf{r}_{d4} - \mathbf{r}_4) + \mathbf{K}_{d4}(\dot{\mathbf{r}}_{d4} - \dot{\mathbf{r}}_4)] \end{aligned} \quad (24)$$

Here, $\tilde{\mathbf{J}}_{2y}^T$ is the second column vector that comprises $\tilde{\mathbf{J}}_2^T$ defined in Eq.(4). K_{p2y} and K_{d2y} are control gains of position y_{d2} and velocity \dot{y}_{d2} in y axis direction in Σ_W of 2nd link that is shown in Fig.2 and Fig.14, \mathbf{J}_4 is Jacobian matrix defined by Eq.(4) when $n = 4$, and \mathbf{K}_{p4} and \mathbf{K}_{d4} are control gain matrices of position and velocity.

Eq.(23) can be realizable in the case that robots are driven by Direct Drive motors, but usual DC motor is driven by voltage input. In this report, the following equation that gives input voltage \mathbf{v} to the DC motors is used instead of a controller of Eq.(23), where \mathbf{K}_v is coefficient matrix to convert torque into voltage.

$$\mathbf{v} = \mathbf{K}_v [\mathbf{B}^+(\mathbf{a} - \mathbf{A}f_{n2d}) + (\mathbf{I} - \mathbf{B}^+\mathbf{B})\boldsymbol{p}] \quad (25)$$

4. Simulation of Tracking Hand Trajectory

4.1. Conditions

In this section, the position/force control performances of 4 links manipulator shown in Fig. 2 through input voltage \mathbf{v} given by Eq.(25) are discussed.

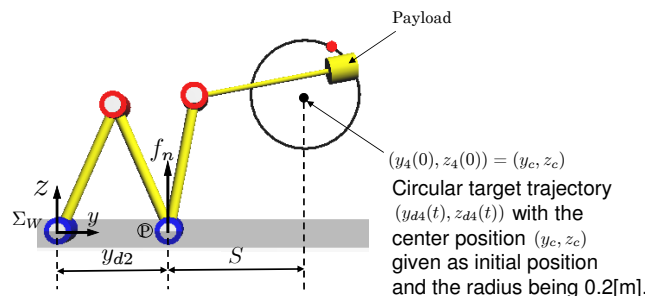


Fig. 2 Simulation model

Link's mass is $m_i = 1.0$ [kg], link's length is $l_i = 0.5$ [m], viscous friction coefficient of joint is $D_i = 2.9$ [N · m · s/rad], torque constant is $K_i = 0.2$ [N · m/A], resistance is $R_i = 0.6$ [Ω], inductance is $L_i = 0.1$ [H], inertia moment of motor is $I_{mi} = 1.64 \times 10^{-4}$ [kg · m²], reduction ratio is $k_i = 3.0$ and viscous friction coefficient of reducer is $d_{mi} = 0.1$ [N · m · s/rad] ($i = 1, 2, 3, 4$).

Desired hand trajectory \mathbf{r}_{d4} includes $y_{d4}(t)$, $z_{d4}(t)$ and desired reaction force f_{n2d} in to the controller Eq.(24) is given as follows.

$$y_{d4}(t) = 0.2 \cos \frac{2\pi}{10}t + y_c \tag{26}$$

$$z_{d4}(t) = 0.2 \sin \frac{2\pi}{10}t + z_c \tag{27}$$

$$f_{n2d} = 30[N] \tag{28}$$

Considering that total weight of links is 4[kg], we set $f_{n2d} = 30[N]$ for a desired value of constraint force. And all the simulations in section 4 use the above basic conditions.

4.2. Energy Consumption Performance

In this section, effectiveness of bracing elbow is evaluated. Energy consumption and accuracy of hand control are used as evaluation indices. Energy consumption of i-th link of manipulator is represented as the following equations during time $0 \sim T$ [s].

$$E_i(T) = \int_0^T v_i(t) i_i(t) dt \tag{29}$$

$$E(T) = \sum_{i=1}^4 E_i(T) \tag{30}$$

Here, the second link is assumed as an elbow. The motions that an elbow of manipulator is subject to constraint and is not subject to constraint are compared. Center coordinate of target trajectory in Fig.2 is $(y_c, z_c) = (0.9, 0.5)[m]$, initial hand position is $(0.9, 0.5)[m]$ and initial bracing position is $(0.4, 0)[m]$. Graphs of hand trajectory and energy consumption from $t = 0[s]$ to $t = T = 30[s]$ in the case that the elbow is subject to constraint and is not subject to constraint are shown in Figs.3 and 4.

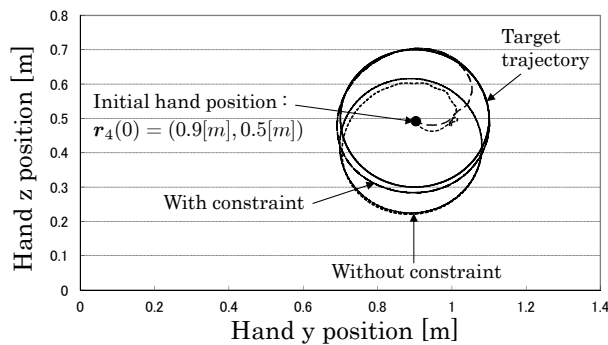


Fig. 3 Position time profile of hand

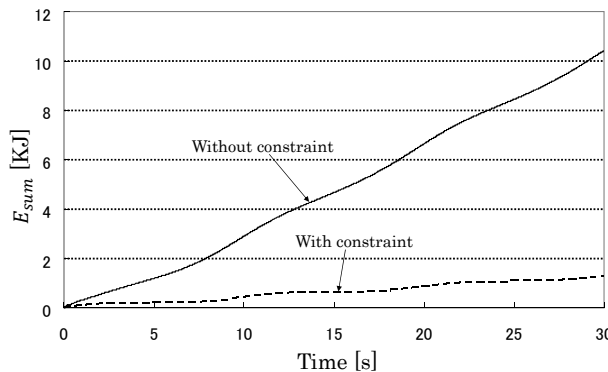


Fig. 4 Comparison of energy consumption defined by Eq.(30)

From Fig.3, the accuracy of hand trajectory is improved by bracing elbow. And Fig.4, energy consumption is reduced by one tenth comparing bracing elbow with no bracing, which displays the drastic effectiveness of bracing elbow.

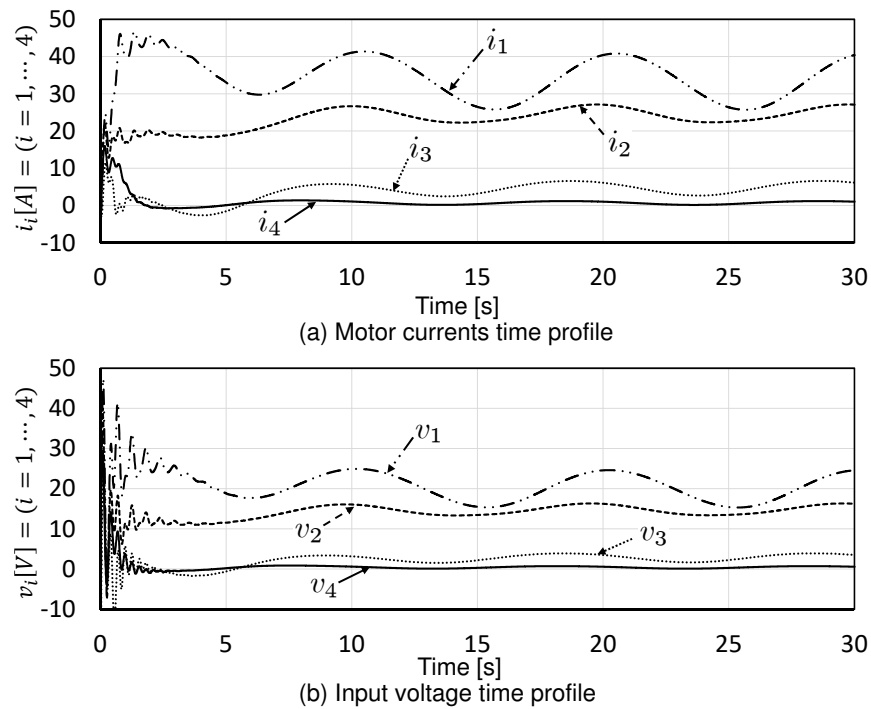


Fig. 5 Input voltages and currents of motors without bracing

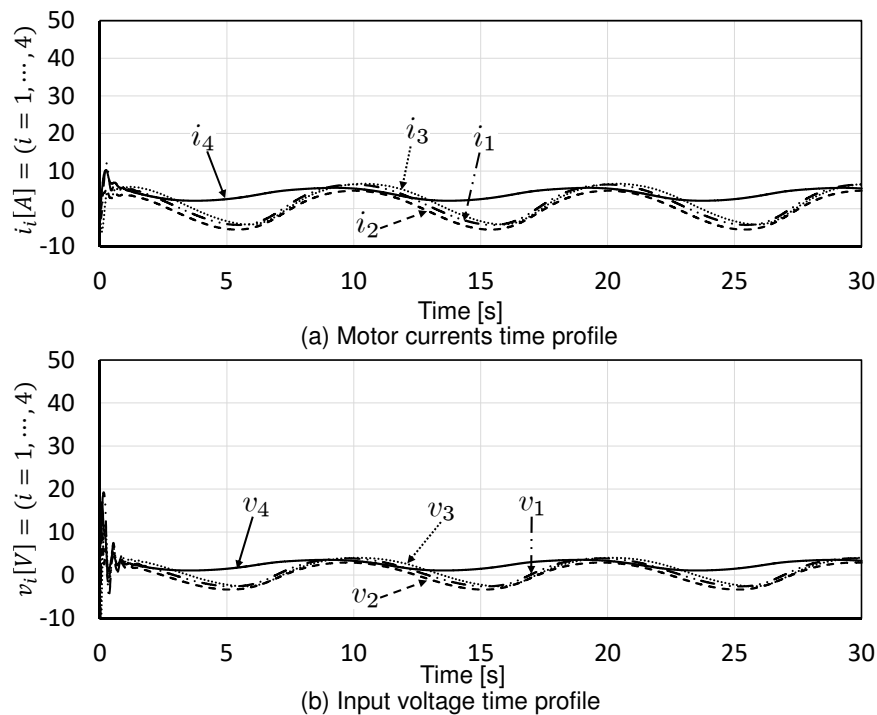


Fig. 6 Input voltages and currents of motors with 2nd link bracing

Fig.5 depicts (a) Motor currents and (b) motor voltages from $t = 0$ to $t = 30[s]$ in the case of not bracing elbow. From the figure, transient response is observed after $t = 0$. Motor currents and voltages in the case of bracing elbow is shown in Fig.6 to compare with the motion of no bracing results in Fig.5. Motor current of first joint in Fig.6(a) i_1 is about one tenth the ampere less than the case of no bracing elbow in Fig.5(a). Motor voltage of first joint v_1 in Fig.5(b) is about one seventh less than the case of no bracing elbow. The differences of links ($i = 2, 3, 4$) are less than the results of the first link.

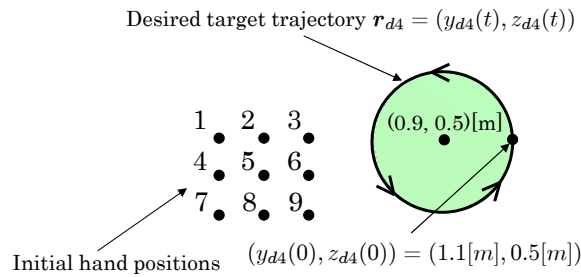


Fig. 7 Initial hand positions

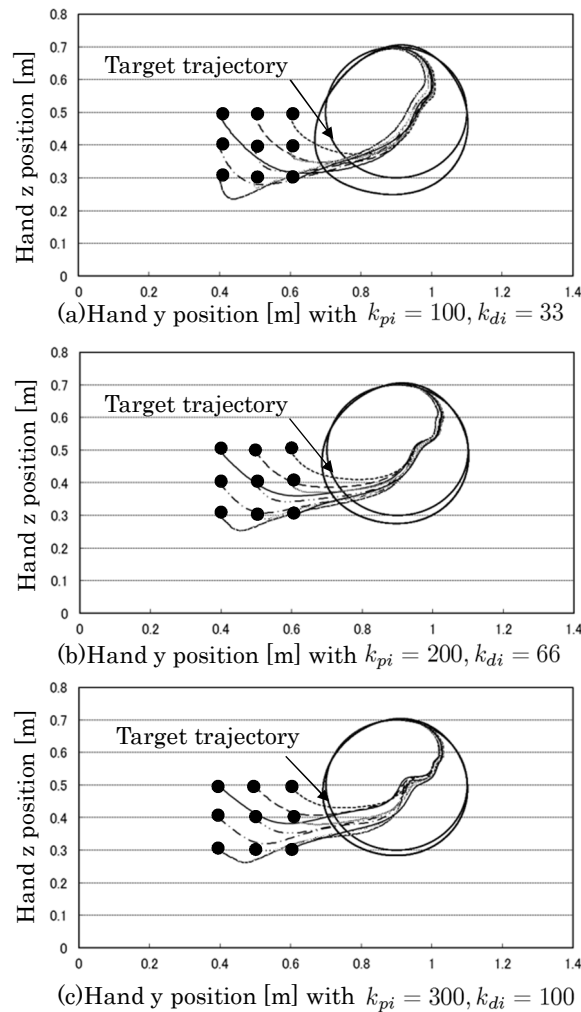


Fig. 8 Position time profiles of hand with constraint

4.3. Trajectory Tracking Performances

A Target trajectory of hand and the initial positions are shown in Fig.7. Nine positions as initial hand position are prepared. The y_{d2} in Eq.(24) is set at 0.4[m], f_{n2d} in Eq.(23) is 30[N]. Gains are $\mathbf{K}_{p4} = \text{diag}[300, 300][N/m]$, $\mathbf{K}_{d4} = \text{diag}[100, 100][Ns/m]$, $K_{p2y} = 150 [N/m]$ and $K_{d2y} = 75 [Ns/m]$. Initial elbow bracing position is (0.4,0.0)[m] in all cases, where the initial positions of the hand are 1: (0.4, 0.5), 2: (0.5, 0.5), 3: (0.6, 0.5), 4: (0.4, 0.4), 5: (0.5, 0.4), 6: (0.6, 0.4), 7: (0.4, 0.3), 8: (0.5, 0.3), 9: (0.6, 0.3)[m], and are given as illustrated in Fig.7.

Trajectory tracking results with bracing elbow are shown in Fig.8 to compare the results to those with not bracing elbow shown by Fig.9, whose gain settings are (a): $k_{pi} = 100, k_{di} = 33$, (b): $k_{pi} = 200, k_{di} = 66$, (c): $k_{pi} = 300, k_{di} = 100$. In all these cases, a control law of Eq.(25) is used.

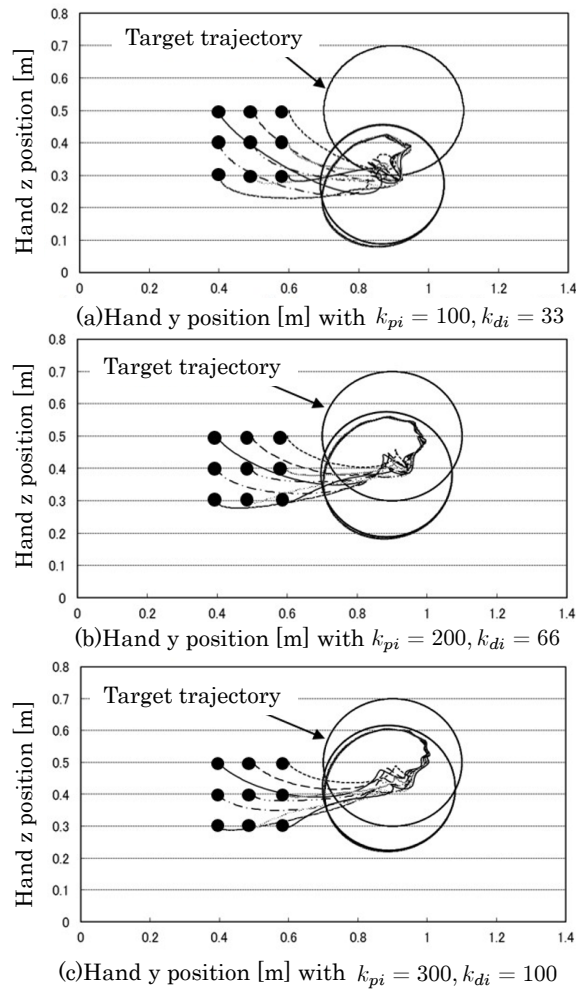


Fig. 9 Position time profiles of hand without constraint

4.4. Configuration Control Performances

In the case of no constraint condition in Fig.9, because $\partial C/\partial \mathbf{q}^T$ is null matrix, \mathbf{B} is equal to $\mathbf{0}$. Then from Eq.(23), $\boldsymbol{\tau}$ resulted in being equal to \mathbf{p} . And concerning Eq.(24), because a part of controlling elbow bracing position does not exist, the first term of the right side disappears. Substituting the result of $\mathbf{p} = \mathbf{J}_4^T[\mathbf{K}_{p4}(\mathbf{r}_{d4} - \mathbf{r}_4) + \mathbf{K}_{d4}(\dot{\mathbf{r}}_{d4} - \dot{\mathbf{r}}_4)]$ in Eq.(25) that is $\mathbf{v} = \mathbf{K}_v \mathbf{p}$ since $\mathbf{B} = 0$, we get the following equation.

$$\mathbf{v} = \mathbf{K}_v[\mathbf{J}_4^T(\mathbf{K}_{p4}(\mathbf{r}_{d4} - \mathbf{r}_4) + \mathbf{K}_{d4}(\dot{\mathbf{r}}_{d4} - \dot{\mathbf{r}}_4))] \tag{31}$$

This result reveals that the control strategy for constraint motion represented by Eqs.(24) and (25) is consistent with the well-known world coordinate control scheme using Jacobian transpose described by Eq.(31). Then all conditions given to the simulations of Fig.8 is identical with conditions of Fig.9, except the conditions of bracing in Fig.8 and no bracing in Fig.9. From Figs.8 and 9, error of tracking trajectory with no bracing in Fig.9 is obviously bigger than those in Fig.8 and the motion of bracing elbow has advantages.

Fig.10 shows transitions of the manipulator's configuration of (a) with constraint and (b) without constraint - each is corresponding to Fig.8 and Fig.9 — in the case that motion of tracking target trajectory start from the initial hand position “1” in Fig.7. In Fig.10(b), the manipulator's configuration changes widely from depicted in (a). This occurred because the control strategy in Eq.(31) does not refer to the manipulator's configuration. In contrast Fig.10(a), the manipulator's configuration did not change widely by bracing elbow, although the controller described by Eqs.(24) and (25) did not specify explicitly manipulator's configuration.

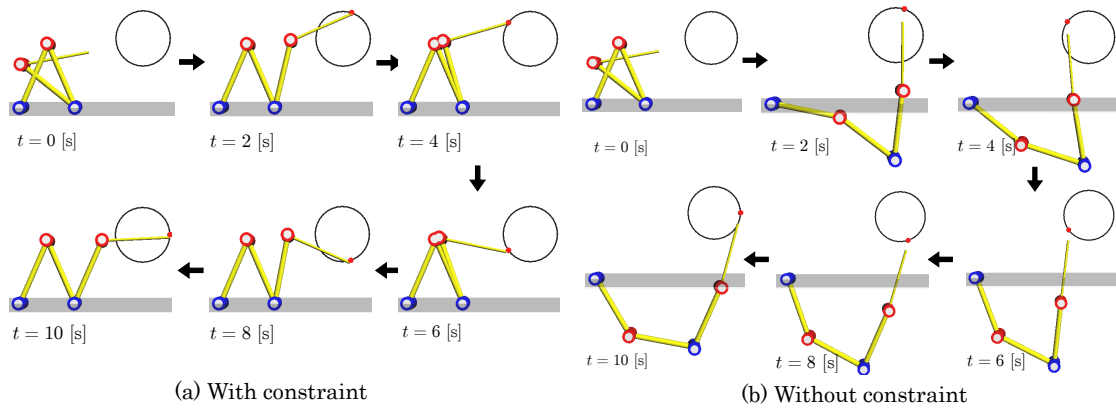


Fig. 10 Time-Profile transition of the manipulator's configuration

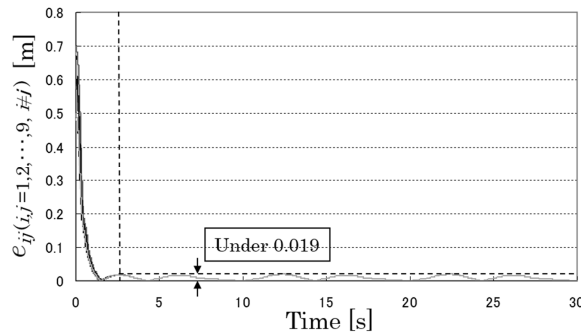


Fig. 11 Error of the hand

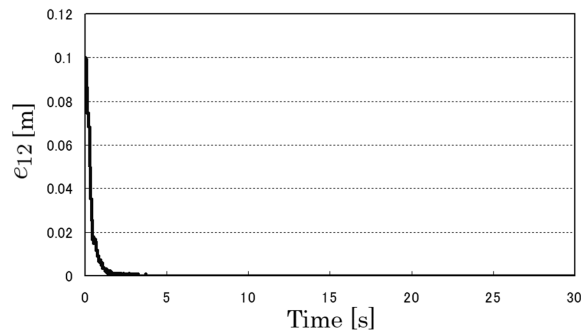


Fig. 12 Error profile between the trajectory started from initial point 1 in Fig.7 and the trajectory started from point 2

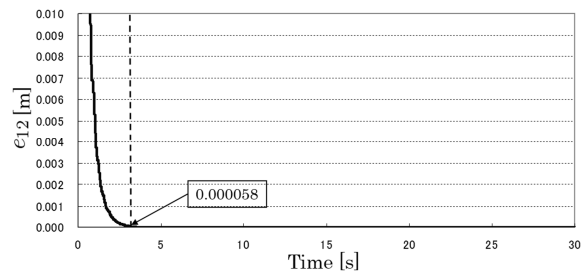


Fig. 13 Expanded error profile in Fig.12

4.5. Convergence of Trajectory

Here, Error $e(t)$ between a target trajectory and hand trajectory is defined as the following equation.

$$e(t) = \sqrt{(y_{d4} - y_4)^2 + (z_{d4} - z_4)^2} \tag{32}$$

Errors between hand trajectories started from i -th initial positions depicted in Fig.7 and j -th ones are defined as the following equation.

$$e_{ij}(t) = \sqrt{(y_{4i} - y_{4j})^2 + (z_{4i} - z_{4j})^2} \quad (33)$$

$(i, j = 1, 2, \dots, 9, i \neq j)$

Applying to the same nonconstraint condition in Fig.10(b), the errors between hand trajectories started from i -th and j -th in initial positions are almost overlapping and all are less than 0.019[m] after 3[s] as shown in Fig.11. Considering constraint condition in Fig.10(a), the error $e_{12}(t)$ of trajectory started from points “1” and “2” is shown in Fig.12, and an extended figure of the vertical-axis of Fig.12 is shown in Fig.13. The error is less than 5.8×10^{-5} after 3[s]. Cases of other errors of trajectories between i -th and j -th starting position ($i \neq j$) in Fig.7 are the same, so there seems to be no effect for the difference of initial values after 3[s] from the start.

4.6. Optimization of Elbow Bracing Position

In this section, optimization of elbow bracing position is discussed. From previous simulation, because it has been confirmed that there is no meaningful difference of initial positions after 3[s] by Figs.11-13, elbow bracing position is discussed in this section from a view point of optimization of energy consumption $E^*(T)$ after $t = 3$ [s] defined by following Eqs.(34) and (35),

$$E_i^*(T) = \int_3^T v_i(t) i_i(t) dt, \quad (34)$$

$$E^*(T) = \sum_{i=1}^4 E_i^*(T). \quad (35)$$

M , mass of hand’s payloads, is changed as 0.0, 0.2, \dots , 1.2[kg]. Central coordinates (y_c, z_c) of circular target trajectory shown in Fig.2 are defined as Eq.(36), and the three cases are named as A, B and C as shown in Fig.14. Target bracing position y_{d2} in Eq.(24) and initial bracing position $y_2(0)$ are shown as figures from w_1 to w_{17} in Fig.15. Because initial hand position $(y(0), z(0))$ is set at central coordinates of circular target trajectory, we set initial hand position for case “A” as (0.8,0.5), for case “B” as (0.9,0.5) and for case “C” as (1.0,0.5) as shown below and in Fig.14, for each bracing position variety form w_1 to w_{17} .

$$(y_c, z_c) = \begin{cases} (0.8, 0.5) : \text{case A} \\ (0.9, 0.5) : \text{case B} \\ (1.0, 0.5) : \text{case C} \end{cases} \quad (36)$$

Where the $E^*(T)$ in Eq.(35) in each case A~C are examined with bracing position varieties shown in Fig.15.

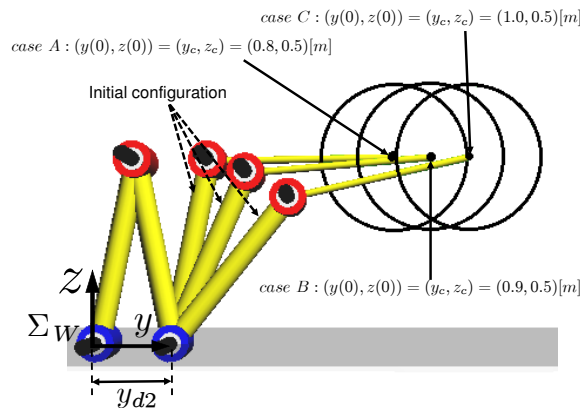


Fig. 14 Circular target trajectory and initial configuration of case A, B and C

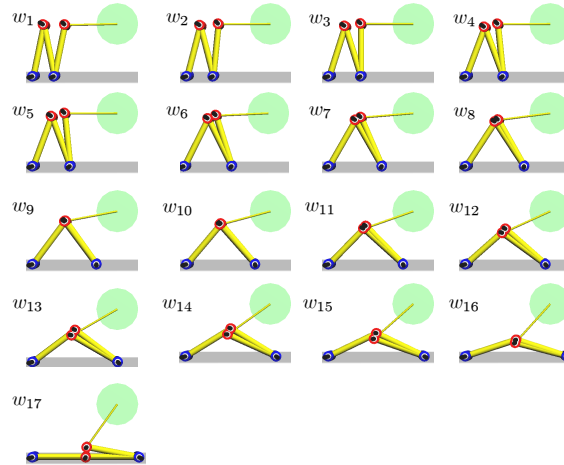


Fig. 15 Desired elbow-bracing position in simulation: $w_1 : y_{d2} = y_2(0) = 0.20$, $w_2 : y_{d2} = y_2(0) = 0.25$
 $w_3 : y_{d2} = y_2(0) = 0.30$, $w_4 : y_{d2} = y_2(0) = 0.35$ $w_5 : y_{d2} = y_2(0) = 0.40$, $w_6 : y_{d2} = y_2(0) = 0.45$
 $w_7 : y_{d2} = y_2(0) = 0.50$, $w_8 : y_{d2} = y_2(0) = 0.55$ $w_9 : y_{d2} = y_2(0) = 0.60$, $w_{10} : y_{d2} = y_2(0) = 0.65$
 $w_{11} : y_{d2} = y_2(0) = 0.70$, $w_{12} : y_{d2} = y_2(0) = 0.75$ $w_{13} : y_{d2} = y_2(0) = 0.80$, $w_{14} : y_{d2} = y_2(0) = 0.85$
 $w_{15} : y_{d2} = y_2(0) = 0.90$, $w_{16} : y_{d2} = y_2(0) = 0.95$ $w_{17} : y_{d2} = y_2(0) = 1.00$, where y_{d2} is given by Eq.(24)

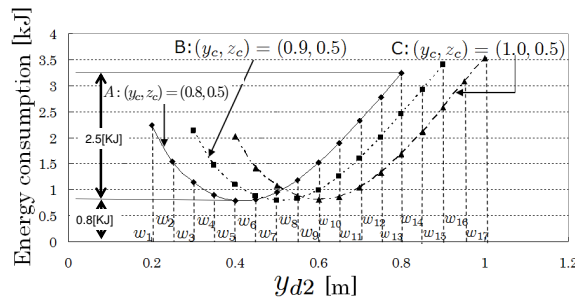


Fig. 16 Evaluation of energy consumption($M=0.0$)

Fig.16 depicts energy consumptions with a condition that hand's payload, M is zero, and the vertical axis shows energy consumption $E^*(T)$ that is calculated by Eq.(35). The horizontal axis in the figure represents a bracing point distance y_{d2} from a origin of Σ_W to bracing position shown in Fig.2, whose $y_{d2} = 0.2$ corresponds to the configuration w_1 in Fig.15. In Fig.16, $w_1 \sim w_{17}$ depicted in the horizontal axis correspond to $w_1 \sim w_{17}$ in Fig.15. A, B and C in Fig.16 correspond to the case A, B and C that show the varieties of the center positions of target circular trajectory whose center positions are defined by Eq.(36) and depicted in Fig.14. Fig.16 reveals that optimal bracing positions are 0.4, 0.5 and 0.6[m] in each case of A, B and C. From Fig.16, as the center coordinates of target trajectory move to positive direction of y axis like A, B and C, optimal bracing position also move to positive direction of y axis.

Next, the mass M of object that is attached on the hand is increased from 0.2[kg] to 1.2[kg] in steps of 0.2[kg], and simulations are conducted by changing bracing position shown in Fig.15 for each cases. Graphs of energy consumption by changing bracing position and center coordinate as parameters are shown in Figs.17-22.

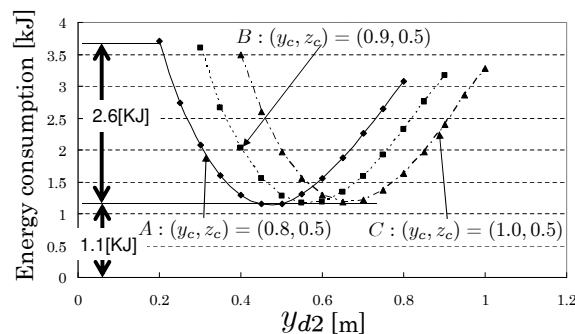


Fig. 17 Evaluation of energy consumption($M=0.2$)

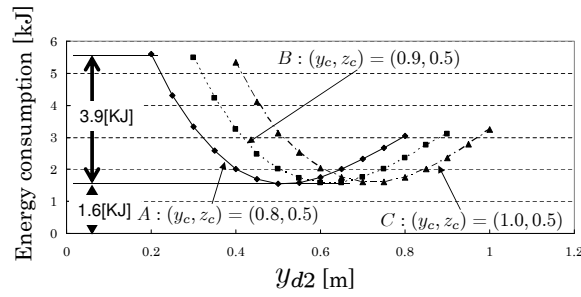


Fig. 18 Evaluation of energy consumption($M=0.4$)

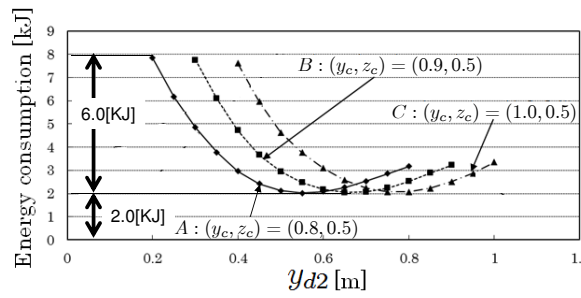


Fig. 19 Evaluation of energy consumption($M=0.6$)

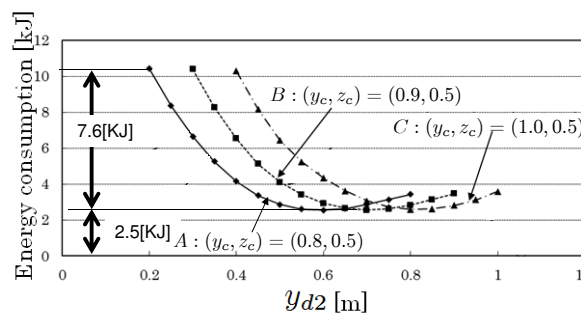


Fig. 20 Evaluation of energy consumption($M=0.8$)

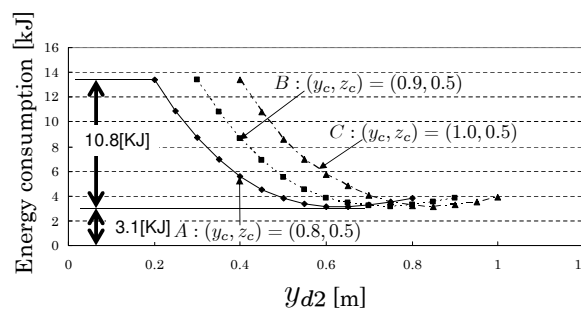


Fig. 21 Evaluation of energy consumption($M=1.0$)

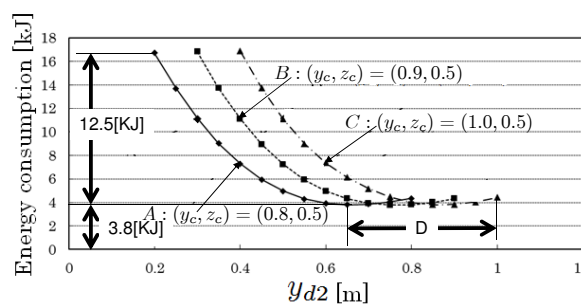


Fig. 22 Evaluation of energy consumption($M=1.2$)

Here, the distance between the center coordinates and the bracing position is defined as S in Fig.2, and S is equal to $y_c - y_{d2}$. Optimal bracing position S in the case that the center coordinate is given as A, is calculated as $S = 0.8 - 0.4 = 0.4$ [m] in Fig.16. In Fig.17, because energy consumption is lowest in $y_{d2} = 0.45$, $S = 0.8 - 0.45 = 0.35$. From Figs.16-22, S are 0.40 [m]($M = 0.0$ [kg]), 0.35 [m]($M = 0.2$ [kg]), 0.30 [m]($M = 0.4$ [kg]), 0.25 [m]($M = 0.6$ [kg]), 0.20 [m]($M = 0.8$ [kg]), 0.15 [m]($M = 1.0$ [kg]) and 0.15 [m]($M = 1.2$ [kg]). Above results represents the fact that as hand's payload increases, energy consumption can be reduced with the elbow bracing point coming closer to the center position of the target trajectory.

The forms of graphs of energy consumptions in Figs.16-22 are horseshoe shape, and in the case that bracing position is too near to target trajectory, energy consumption increase. From Figs.16-22, as hand's payload increases, it is difficult to discriminate optimal bracing position, for example, a section marked "D" in Fig.22. Moreover, from Fig.16, minimum energy consumption in the case of $M = 0$ [kg] is 0.8 [kJ] regardless of A, B and C. From Fig.17, minimum energy consumption is 1.1 [kJ]($M = 0.2$ [kg]), and from Fig.18, minimum energy consumption is 1.6 [kJ]($M = 0.4$ [kg]). Similarly, minimum energy consumptions are 2.0 [kJ]($M = 0.6$ [kg]), 2.5 [kJ]($M = 0.8$ [kg]), 3.1 [kJ]($M = 1.0$ [kg]) and 3.8 [kJ]($M = 1.2$ [kg]) as shown in Figs.19-22. From the above results, it is found that as hand's payload increases, minimum energy consumption also increases.

From Figs.16-22, when bracing position y_{d2} moves from $w_1 : 0.2$ to $w_{17} : 1.0$, the difference between maximum and minimum energy consumption increases as hand's payload increasing. For example, when $M = 0$ [kg], the difference is 2.5 [kJ] in case of A as shown in Fig.16, and when $M = 1.2$ [kg], the difference is 12.5 [kJ] as shown in Fig.22. Therefore the tendency that the difference of energy consumption depends on bracing position is so noticeable as hand's payload increases, and the effect of optimizing bracing position is so effective and meaningful as grasping payload increases.

5. Conclusion

In this paper, firstly advantages of constraint motion regarding accuracy of hand trajectory tracking was considered by comparing motions of bracing elbow with motions of no bracing. Then, the merits of bracing that accuracy of tracking trajectory can be improved and energy consumptions be reduced by bracing elbow are shown. Moreover, the tendencies that bracing positions that minimize energy consumption alters depending on position of target trajectory and weight of hand's payload have been unveiled. In the future, we will try to optimize online bracing position based on the results of this paper.

References

- Chirikjian, G. S. and Burdick, J. W., A Hyper-Redundant Manipulator, IEEE Robotics and Automation Magazine, (1994), pp.22-29.
- Glass, K., Colbaugh R., Lim, D. and Seraji, H., Real-time collision avoidance for redundant manipulators, IEEE Trans. on Robotics and Automation, Vol.11 (1995), pp.448-457.
- Hemami, H. and Wyman, B. F., Modeling and Control of Constrained Dynamic Systems with Application to Biped Locomotion in the Frontal Plane, IEEE Trans. on Automatic Control, Vol.AC-24, No.4 (1979), pp.526-535.
- Hirose, S. and Chu, R., Development of a light weight torque limiting M-Drive actuator for hyper-redundant manipulator Float Arm, Robotics and Automation, Proc. of IEEE International Conference, Vol.4 (1999), pp.2831-2836.
- Kondo, D., Itosima, M., Minami, M. and Yanou, A., Proposal of Bracing Controller Utilizing Constraint Redundancy and Optimization of Bracing Position, Proceedings of SICE Annual Conference, (2013), pp.2732-2737.
- Minami, M., Asakura, T., Dong, L. X. and Huang, Y. M., Position Control and Explicit Force Control of A Constrained Manipulator, IEEE Int. Conf. on Intelligent Processing System, (1997), pp.1268-1271.
- Minami, M. and Xu, W., Shape-grinding by Direct Position / Force Control with On-line Constraint Estimation, IEEE/RSJ International Conference on Intelligent Robots and Systems (IROS), (2008), pp. 943-948.
- Minami, M., Tanimoto, H., Yanou, A. and Takebayashi, M., Continuous Shape-Grinding Experiment based on Constraint-combined Force / Position Hybrid Control Method, SICE Journal of Control, Measurement, and System Integration, Vol.7, No1 (2014), pp.2-11.
- Peng, Z. X. and Adachi, N., Position and Force Control of Manipulators without Using Force Sensors, Trans. of the Japan Society of Mechanical Engineers(C), Vol.57 (1991), pp.1625-1630, (in Japanese).

- Park, J. and Khatib, O., Multi-Link Multi-Contact Force Control for Manipulators, Proc. of 2005 IEEE Int. Conf. on Robotics and Automation, (2005), pp.3624-3629.
- Petrovskaya, A., Park, J. and Khatib, O., Probabilistic Estimation of Whole Body Contacts for Multi-Contact Robot Control, Proc. of IEEE International Conference on Robotics and Automation, (2007), pp.568-573.
- Roy, J. and Whitcomb, L. L., Adaptive Force Control of Position/Velocity Controlled Robots, Theory and Experiment, IEEE Transactions on Robotics and Automation, Vol.18, No.2 (2002), pp.121-137.
- Schutter, J. D. and Brussel, H. V., Compliant robot motion 2. A control approach based on external control loops, Int. J. Robot. Res., Vol.7, No.4 (1988), pp.18-33.
- Siciliano, B. and Villani, L., A passivity-based approach to force regulation and motion control of robot manipulators, Automatica, Vol.32, No.3 (1996), pp.443-447.
- Seraji, H. and Bon, B., Real-Time Collision Avoidance for Position-Controlled Manipulators, IEEE Trans. on Robotics and Automation, Vol.15, No.4 (1999), pp.670-677.
- Villani, L., de Wit, C. C. and Brogliato, B., An exponentially stable adaptive control for force and position tracking of robot manipulators, IEEE Trans. Automat. Contr., Vol44 (1999), pp.778-802.
- West, H. and Asada, H., A Method for the Design of Hybrid Position/Force Controllers for Manipulators Constrained by Contact with the Environment, Proc. of IEEE Int. Conf. on Robotics and Automation, (1985), pp.251-260.
- Washino, Y., Minami, M., Kataoka, H., Matsuno, T., Yanou, A., Itoshima, M. and Kobayashi, Y., Hand- Trajectory Tracking Control with Bracing Utilization of Mobile Redundant Manipulator, SICE Annual Conference, (2012), pp.219-224.
- Yoshikawa, T., Dynamic Hybrid Position/Force control of Robot Manipulators—Description of Hand Constraints and Calculation of Joint Driving Force, IEEE J. on Robotics and Automation, Vol.RA-3, No.5 (1987), pp.386-392.
- Yamane, K. and Nakamura, Y., Forward Dynamics Computation of Open Kinematic Chains Based on the Principle of Virtual Work, Proc. of IEEE Int. Conf. on Robotics and Automation, (2001), pp.2824-2831.
- Yamane, K. and Nakamura, Y., Dynamics Filter - Concept and Implementation of On-Line Motion Generator for Human Figures, IEEE Transactions on Robotics and Automation, vol.19, No.3 (2003), pp.421-432.